Cancer Stem Cells Contribute to Cisplatin Resistance in *Brca1/p53*–Mediated Mouse Mammary Tumors

Norazizah Shafee,[1] Christopher R. Smith,[2] Shuanzeng Wei,[2] Yoon Kim,[2] Gordon B. Mills,[3,4] Gabriel N. Hortobagyi,[4] Eric J. Stanbridge,[1] and Eva Y-H. P. Lee[2]

Departments of [1]Microbiology and Molecular Genetics and [2]Biological Chemistry and Developmental and Cell Biology, College of Medicine, University of California, Irvine, California; and Departments of [3]System Biology and [4]Breast Medical Oncology, University of Texas M. D. Anderson Cancer Center, Houston, Texas

Abstract

The majority of *BRCA1*-associated breast cancers are basal cell–like, which is associated with a poor outcome. Using a spontaneous mouse mammary tumor model, we show that platinum compounds, which generate DNA breaks during the repair process, are more effective than doxorubicin in *Brca1/p53*–mutated tumors. At 0.5 mg/kg of daily cisplatin treatment, 80% primary tumors ($n = 8$) show complete pathologic response. At greater dosages, 100% show complete response ($n = 19$). However, after 2 to 3 months of complete remission following platinum treatment, tumors relapse and become refractory to successive rounds of treatment. Approximately 3.8% to 8.0% (mean, 5.9%) of tumor cells express the normal mammary stem cell markers, CD29^{hi}24^{med}, and these cells are tumorigenic, whereas CD29^{med}24$^{-/lo}$ and CD29^{med}24^{hi} cells have diminished tumorigenicity or are nontumorigenic, respectively. In partially platinum-responsive primary transplants, 6.6% to 11.0% (mean, 8.8%) tumor cells are CD29^{hi}24^{med}; these populations significantly increase to 16.5% to 29.2% (mean, 22.8%; $P < 0.05$) in platinum-refractory secondary tumor transplants. Further, refractory tumor cells have greater colony-forming ability than the primary transplant–derived cells in the presence of cisplatin. Expression of a normal stem cell marker, *Nanog*, is decreased in the CD29^{hi}24^{med} populations in the secondary transplants. *Top2A* expression is also down-regulated in secondary drug-resistant tumor populations and, in one case, was accompanied by genomic deletion of *Top2A*. These studies identify distinct cancer cell populations for therapeutic targeting in breast cancer and implicate clonal evolution and expansion of cancer stem-like cells as a potential cause of chemoresistance. [Cancer Res 2008;68(9):3243–50]

Introduction

Mutations in breast cancer susceptibility genes *BRCA1* and *BRCA2* and several other genes encoding BRCA1/2-interacting proteins are associated with hereditary breast and ovarian cancer syndrome (reviewed in refs. 1, 2). Hereditary breast cancer accounts for 5% to 10% of all breast cancers, and of these, *BRCA1* mutations

account for approximately half of the cases. In sporadic breast cancer, *BRCA1* mutations are rare; however, significant percentages of sporadic cancers show reduced or absent expression of BRCA1 due to promoter hypermethylation (3). *BRCA1* encodes a 220-kDa nuclear phosphoprotein that contains multiple functional domains that interact with proteins involved in different cellular processes, including ubiquitously expressed tumor suppressors, oncoproteins, DNA damage repair proteins, cell cycle regulators, and transcriptional activators and repressors (reviewed in refs. 4, 5).

In addition to interacting with ubiquitously expressed proteins, BRCA1 associates and regulates ubiquitination of steroid hormone receptors, estrogen receptor α and progesterone receptor (reviewed in ref. 6). Paradoxically, *BRCA1*-associated breast cancers are frequently high-grade, estrogen receptor α/progesterone receptor/ Her2 (triple)–negative basal cell–like tumors (7), with frequent mutations of *TP53* and *PTEN* (8). The triple-negative tumors are initially responsive to chemotherapy with a high percentage entering pathologic complete response; however, tumors that recur or do not enter complete remission progress rapidly, resulting in a poor outcome.

Roles of BRCA1 in both homologous recombination and nonhomologous end joining DNA repair have been shown. Therapeutic strategies that explore the DNA repair defect in BRCA mutants have been proposed and are showing promise, in particular with poly(ADP-ribose) polymerase 1 inhibitors (9). *BRCA1*-mutated cell lines are more sensitive to cisplatin and less responsive to doxorubicin (10, 11). However, the *in vivo* response and long-term effects of platinum-based therapy in *BRCA1*-associated tumors have yet to be established.

Mice carrying somatic mutations of *Brca1* and/or *p53* alleles in mammary epithelial cells using the Cre/loxP system develop mammary tumors with high penetrance (12–15). Tumor latency in *Brca1$^{fp/fp}$p53$^{fp/fp}$WAPCre^c* mice, which express exon 11–deleted Brca1 and exon 5– and exon 6–deleted p53, is slightly shorter than that of *Brca1$^{fp/fp}$p53$^{fp/fp}$CK14Cre^c* mice, which carry null alleles of *Brca1* and *p53* (13, 14). On the other hand, *MMTVCre^a* target a small number of cells in the mammary gland and has much longer tumor latency (12). High tumor penetrance and consistent tumor latency of *Brca1$^{fp/fp}$p53$^{fp/fp}$WAPCre^c* and *p53$^{fp/fp}$WAPCre^c* mice allow studies of therapeutic response to single chemotherapeutic agents such as cisplatin [*cis*-dichlorodiamineplatinum (CDDP)], carboplatin, and doxorubicin, *in vivo*. CDDP is a member of platinum-based compounds that form various intrastrand and interstrand adducts with DNA (reviewed in ref. 16). Repair of the platinum adduct is mediated by nucleotide excision repair and single-strand and double-strand DNA break repair pathways. The clinical use of this drug is limited due to the emergence of intrinsic and acquired resistance and severe peripheral neurotoxicity. Other platinum derivatives, such as carboplatin and oxaliplatin, have

different toxicities and are more commonly used in the clinical setting. Doxorubicin, also known as Adriamycin, is the most widely used anthracycline antibiotic in the treatment of breast cancer. It forms a complex with DNA by intercalation between base pairs, leading to the formation of free radicals and subsequent inhibition of DNA topoisomerase II catalytic activity (17). In clinically aggressive breast cancer, doxorubicin is most lethal to cells that contain high levels of topoisomerase II and are undergoing high rates of DNA replication. Chemotherapy has improved survival rates among cancer patients, but chemoresistance, which results in failure in cancer treatment, remains a major challenge.

There is now much evidence that cancer stem cells, a minority tumor cell population with stem cell properties, are capable of maintaining continuous tumor growth (reviewed in ref. 18). Cancer stem cells were first identified in acute myelogenous leukemia and have recently been shown to be present in many solid tumors, including tumors of the breast, central nervous system, and lung adenocarcinoma (reviewed in ref. 19). In breast cancers, $CD44^+CD24^{-/low}$ putative cancer stem cells were identified (20). In glioblastoma, a population of $CD133^+$ cancer stem cells showed significant resistance to chemotherapeutic agents including temozolomide, carboplatin, paclitaxel, and etoposide (21). In small-cell lung carcinoma, a small population of stem-like cells showing high clonogenic activity and coexpression of *CD44* and multidrug resistance gene, *MDR1*, showed multidrug resistance (22).

Despite the clinical importance of chemoresistance, to date there have been no reports of chemoresistant stem cell populations in breast cancer. Identification and characterization of such a subpopulation of cells will help develop strategies to target these cells. We show here that spontaneous tumors that developed in the conditional *Brca1/p53* knockout mice respond favorably to platinum treatment, but chemoresistance does occur and often emerges over time. Expansion of a subpopulation of cancer stem cells correlates with drug resistance.

Materials and Methods

Generation of *Brca1^{fp/fp}p53^{fp/fp}Cre* mutant mice and spontaneous mammary tumor formation. Generation of *Brca1^{fp/fp}p53^{fp/fp}Cre* and *p53^{fp/fp}Cre* mice has previously been described (12, 13). Briefly, *Brca1* exon 11–floxed (*Brca1^{fp/fp}*) mice were obtained from Dr. Chu-Xia Deng (NIH, Bethesda, MD; ref. 15). *Brca1^{fp/fp}* mice were bred to *p53* exon 5– and exon 6–floxed (*p53^{fp/fp}*) mice to obtain *Brca1^{fp/+}p53^{fp/+}* mice. *Brca1^{fp/fp}p53^{fp/fp}MMTVCre^a* and *Brca1^{fp/fp}p53^{fp/fp}WAPCre^c* mice were generated by crossing the heterozygous floxed mice with *MMTVCre^a* or *WAPrtTACre^c* transgenic mice followed by crosses of heterozygous mice. The *WAPrtTACre^c* transgene expression was detected either before puberty as reported by Lin and colleagues (12) or in doxycycline-treated pregnant mice. Only the former group of mice were analyzed in the current study. PCR reaction was done to confirm exon 11 deletion of *Brca1* gene and exon 5 and 6 deletions of *p53* gene as previously reported (12, 13). The mice were in a C57BL/6 and 129/Sv mixed background. Mice were monitored for palpable tumors weekly. All animal experiments were in accordance with the guidelines of federal law and Institutional Animal Care and Use Committee at the University of California, Irvine.

Doxorubicin, cisplatin, and carboplatin treatment. Animals were treated with doxorubicin, cisplatin, or carboplatin when tumor diameter reached ~0.5 cm. Doxorubicin (Fluka) was prepared at a stock concentration of 58 mg/mL in DMSO and stored at 4°C. Doxorubicin was diluted in 40% polyethylene glycol 400 (PEG-400; Sigma) in saline at the time of treatment. Cisplatin (CDDP; Sigma) was prepared fresh daily in 40% PEG-400 and saline. Stock solution of carboplatin (Sigma) at 10 mg/mL in water was stored at 4°C; dilution in 40% PEG-400 and saline was made at

the time of treatment. CDDP was administered i.p. every other day at 0.5, 1.5, 3, or 6 mg/kg daily for 7 d. Carboplatin was administered i.p. once every 3 d for 15 d at 32.5 or 60 mg/kg; doxorubicin was administered i.p. weekly at 1.25 or 5 mg/kg for 21 d. Tumor growth was monitored by daily caliper measurements in two perpendicular dimensions. Tumor volume (mm³) was calculated according to the formula $(d^2 \times D) / 2$, where d and D represent the shortest and longest diameters, respectively.

Histology and immunohistochemistry. Mice were sacrificed and tissues collected when tumors reached 0.75 to 1 cm³. The tissue was fixed in 4% paraformaldehyde (Sigma-Aldrich) at 4°C overnight followed by paraffin embedding. Paraffin sections were stained with H&E and examined by light microscopy. Immunostaining was done following the protocol described in the Vectastain Elite ABC kit (Vector Laboratories). To retrieve the antigen, slides were heated for 20 min in 10 mmol/L citrate buffer (pH 6.0) in a microwave oven. Caspase-3 (Cell Signaling Technology), phospho-H3 (Upstate), and Rad51 antibodies were used at 1:200, 1:2,000, and 1:50 dilutions, respectively.

Tissue disaggregation and cell preparation. Tumor tissues were processed according to Stingl and colleagues (23) with modifications. Briefly, tumors were minced into ~2-mm³ fragments with sterile scalpels and enzymatically disaggregated for 8 h at 37°C in EpiCult-B medium (StemCell Technologies, Inc.) with 5% fetal bovine serum (FBS), 300 units/mL collagenase, and 100 units/mL hyaluronidase. After centrifugation at $450 \times g$ for 5 min, RBC were removed by pipetting in 0.64% NH_4Cl. Single-cell suspensions were obtained by sequential pipetting for 1 to 2 min in 0.25% trypsin, followed by 2 min in 5 mg/mL dispase II plus 0.1 mg/mL DNase I (Sigma). The resulting suspension was then filtered through a 40-μm mesh and subjected to removal of lineage positive cells using anti-CD45, anti-TER119, and anti-CD31 antibodies to eliminate hematopoietic and endothelial cells. Magnetic beads were used to enrich mammary epithelial cells using the Mouse Mammary Stem Cell Enrichment Kit according to the manufacturer's protocol (StemCell Technologies). Following the enrichment step, the resulting cell suspension was kept on ice until use.

Cell labeling, flow cytometry, and sorting. Antibody staining was done in PBS supplemented with 1% bovine serum albumin (BSA). Cells were first incubated with 1% BSA for 20 min at a cell concentration of 1×10^6/mL. Cells were subsequently washed and stained with different conjugated antibodies for 30 min, at dilutions predetermined by titration experiments. Antibodies used in this study were antimouse CD24-phycoerythrin (clone M1/69; BD Biosciences) and antimouse CD29-FITC (clone Ha2/5; BD Biosciences). Following removal of excess unbound antibodies by washing twice in PBS, the cells were resuspended in sorting buffer containing 1% BSA and 1 mmol/L EDTA in PBS. The stained cells were subjected to filtration through a 40-μm mesh and kept on ice until sorted. Flow cytometry analysis and sorting was done with the MoFlo flow cytometer (DakoCytomation). Forward scatter area versus forward scatter width profiles were used to eliminate dead cells and cell doublets. Sorting was done to achieve a final average purity of >95%.

Mammary gland transplantation. The no. 4 inguinal mammary gland outgrowths, between nipple and lymph node, of $Rag1^{-/-}$ (The Jackson Laboratory) recipient mice were removed at 3 wk of age. Sorted cells were spun down by low-speed centrifugation ($850 \times g$ for 5 min) and resuspended in DMEM supplemented with 10% FBS and 2 mmol/L L-glutamine. In all experiments, cell number and viability were confirmed with the trypan blue dye exclusion test. Dilutions were done to achieve the required number of viable cells for appropriate injection doses. Cells were then mixed with BD Matrigel (BD Biosciences) at a 1:1 ratio and injected into cleared mammary fat pads of 6- to 8-wk-old $Rag1^{-/-}$ recipient mice. To minimize experimental variability due to potential differences in recipient mice, control cell populations sorted by fluorescence-activated cell sorting (FACS) were injected into the opposite flank of each animal.

***In vitro* epithelial progenitor assays.** The colony-forming ability of mammary epithelial progenitors was determined as previously described (23–25). Sorted cells were cultured onto preseeded feeder layers, prepared from irradiated (5×10^3 cGy) NIH 3T3 cells, at a clonal density of ~800/cm², in EpiCult-B medium (StemCell Technologies) supplemented with 5% FBS. After 24 h, the medium was replaced with serum-free EpiCult-B

medium. In cases where CDDP was used, a predetermined GI_{50} value was added to the culture for 48 h. Five to seven days later, cell colonies were fixed with acetone/methanol (1:1), stained with Giemsa, and counted. Colonies were counted from three replicate experiments and tabulated as the average number of colonies per 100 primary cells.

Embryonic stem cell culture. E14 embryonic stem cell line was cultured as described (26). Total RNA was prepared for reverse transcription-PCR (RT-PCR) and used as a positive control for Oct4 expression.

PCR and RT-PCR. Semiquantitative PCR reactions were done with 100 ng of genomic DNA as template in a mixture containing 20 pmol of each gene-specific primer. The PCR cycling conditions were done with an initial denaturation step at 95°C for 1 min, followed by 35 cycles of 40 s at 94°C for denaturation, 40 s at 60°C for annealing, and 1-min extension at 72°C, followed by a final extension at 72°C for 7 min. Semiquantitative RT-PCR analysis of total RNAs was done with the MasterAmp RT-PCR Kit (Epicentre Biotechnologies). Fifty nanograms of total RNA were used as templates for a first strand synthesis at 60°C for 20 min. This single-tube reaction was then subjected to 40 cycles of denaturation at 95°C for 40 s, annealing at 60°C for 40 s, and extension at 71°C for 1 min with a final extension of 7 min at 72°C. Alternatively, 200 ng of total RNA were reverse transcribed into cDNA using Oligo dT primer and the ImProm-II Reverse Transcription System (Promega) according to the manufacturer's protocol. The resulting single-strand cDNAs (1 μL) were either added to 25 μL of PCR reaction or stored at −20°C. Primer sequences are listed in Supplementary Table S1.

Statistical analysis. Results are presented as the mean ± SD for at least three repeated individual experiments for each group. Analyses were done with the SPSS software. The percentages tumor-free mice were generated using Kaplan-Meier survival curves. Analyses were done with GraphPad Prism software, which combines the log-rank (Mantel-Cox) test and the Gehan-Breslow-Wilcoxon method.

Results and Discussion

To investigate whether *Brca1* mutation alters tumor chemotherapy response *in vivo*, we established *p53*- and *Brca1/p53*–mutant mammary tumor models, respectively, using the Cre/loxP system (12, 13). Nulliparous *Brca1$^{fp/fp}$p53$^{fp/fp}$MMTVCre^a* females developed mammary tumors with complete penetrance (11 of 11) between 11.8 and 16.7 months of age, with a median tumor latency of 14.1 months, as compared with nulliparous *p53$^{fp/fp}$MMTVCre^a* females (n = 18), which developed tumors with a median tumor latency of 16.9 months (P < 0.0001; Fig. 1A). Expression of *MMTVCre^a* is restricted to a small number of cells in the mammary gland (12). As previously shown, mammary tumor latency varied depending partly on the numbers of targeted cells. In nulliparous *Brca1$^{fp/fp}$p53$^{fp/fp}$WAPCre^c* mice, mammary tumors developed between 3.7 and 9.5 months of age, with a median tumor latency of 6.3 months and complete penetrance (39 of 39 mice), as compared with nulliparous *p53$^{fp/fp}$WAPCre^c* mice (n = 18), which have a median tumor latency of 10.6 months (P < 0.0001; Fig. 1A). The median tumor latency in *Brca1$^{fp/fp}$p53$^{fp/fp}$K14Cre^c* mice, described by Liu and colleagues (14), is ∼7.0 months. Thus, double knockout mouse strains harboring *WAPCre^c* have a slightly shorter median tumor latency compared with *K14Cre* mice. Whether this is due to the usage of different promoters or the expression of mutant p53 and BRCA1 proteins in our models is unclear. In contrast to *MMTVCre^a*, the *WAPCre^c* is expressed in >90% of cells in the adult mammary gland (12). The greater acceleration of tumorigenesis by *Brca1* mutation in *WAPCre^c* mice when compared with *MMTVCre^a* is likely due to paracrine actions on cell proliferation by the larger number of *Brca1/p53*–mutated cells.

Most mammary tumors that develop in mice with *Brca1* and *p53* mutations are either adenocarcinomas or spindle cell carcinomas (Supplementary Data), with the vast majority of tumors being poorly differentiated adenocarcinomas, similar to that of human *BRCA1*-associated tumors. This observation correlates with the previously reported *Brca1$^{fp/fp}$p53$^{fp/fp}$K14Cre^c* mice (14). In *p53$^{fp/fp}$WAPCre^c* mice, soft tissue sarcomas, skin tumors, and osteosarcomas, in addition to mammary tumors, were detected in a small number of mice (data not shown). In contrast, all *Brca1$^{fp/fp}$p53$^{fp/fp}$WAPCre^c* mice developed mammary tumors and only one case of osteosarcoma was found in a cohort of 39 mice. Thus, mutations of the *Brca1* gene greatly shorten tumor latency as well as increase selectivity of mammary tumor development.

Tumor-bearing mice were treated with doxorubicin, CDDP, or carboplatin. *p53$^{fp/fp}$* mouse mammary tumors were refractory to doxorubicin or CDDP treatment at all doses tested (Fig. 1B, top). Conversely, all *Brca1$^{fp/fp}$p53$^{fp/fp}$* mammary tumors (n = 19) responded to an initial cycle of four injections of 1.5, 3, or 6 mg/kg CDDP every other day for 7 days (Fig. 1B, bottom). Sensitivity to CDDP treatment was observed in spontaneous tumors developed in *WAPCre^c*; *MMTVCre^a* mice, or in tumor transplants in *Rag1$^{-/-}$* mice, indicating that *Brca1* mutations render tumor cells sensitive to platinum compounds regardless of which *Cre* transgenic mice are assessed. *Brca1$^{fp/fp}$p53$^{fp/fp}$* mammary tumors were also sensitive to treatment with 32.5 mg/kg (n = 3) or 60 mg/kg (n = 1) carboplatin (data not shown). Taken together, a differential sensitivity of spontaneous *Brca1$^{fp/fp}$p53$^{fp/fp}$* mammary tumors to platinum over doxorubicin was found *in vivo*, consistent with the reported observation in a *BRCA1*-deficient human breast cancer cell line (11).

Sensitivity to platinum treatment (24–48 hours posttreatment) correlated with increased immunostaining of activated caspase-3, which showed cytoplasmic and perinuclear localization (Fig. 1C). Phospho-histone 3 expression, marker of the mitotic phase of the cell cycle, was decreased in CDDP-treated cells (Fig. 1C). Rad51 foci that formed at DNA double-strand breaks were detected 48 hours after CDDP treatment in *p53$^{fp/fp}$* tumors (Fig. 1D). In contrast, no Rad51 foci were detected in *Brca1$^{fp/fp}$p53$^{fp/fp}$* tumors. Thus, lack of homologous recombinational repair correlates with increased cell death and reduced mitotic cells in the favorable response to cisplatin. Recent studies showed that *BRCA*-deficient cancer cells are profoundly sensitized to inhibitors of poly(ADP-ribose) polymerase 1 *in vitro* (9). Poly(ADP-ribose) polymerase 1 binds to ssDNA breaks and may lead to persistent DNA lesions, preventing repair by homologous recombination pathways. Indeed, silencing of *BRCA1* or *BRCA2* network genes in *p53*-deficient, but not *p53*-proficient, cells enhances sensitivity to cisplatin (27). Taken together, *BRCA1* and *p53* deficiency leads to selective sensitivity to specific types of chemotherapeutic drug.

Because with doxorubicin treatment *Brca1$^{fp/fp}$p53$^{fp/fp}$* mammary tumors had only a transient slowing down of tumor growth, subsequent studies focused on CDDP-treated mice. Using a lower CDDP dose (0.5 mg/kg; n = 8), 80% of tumors had complete pathologic response to the initial treatment cycle (Fig. 2A) and 20% had only partial regression for 11 to 12 days followed by rapid growth (data not shown), indicating that there is heterogeneity in the initial cisplatin response at the lower CDDP dosage. Following the initial tumor shrinkage and complete pathologic response, tumors relapsed at the same site ∼2 to 3 months posttreatment. Relapse also occurred in mice treated with higher dosages of CDDP (data not shown). To address whether recurrent tumors remain sensitive to platinum compounds, a second round of cisplatin
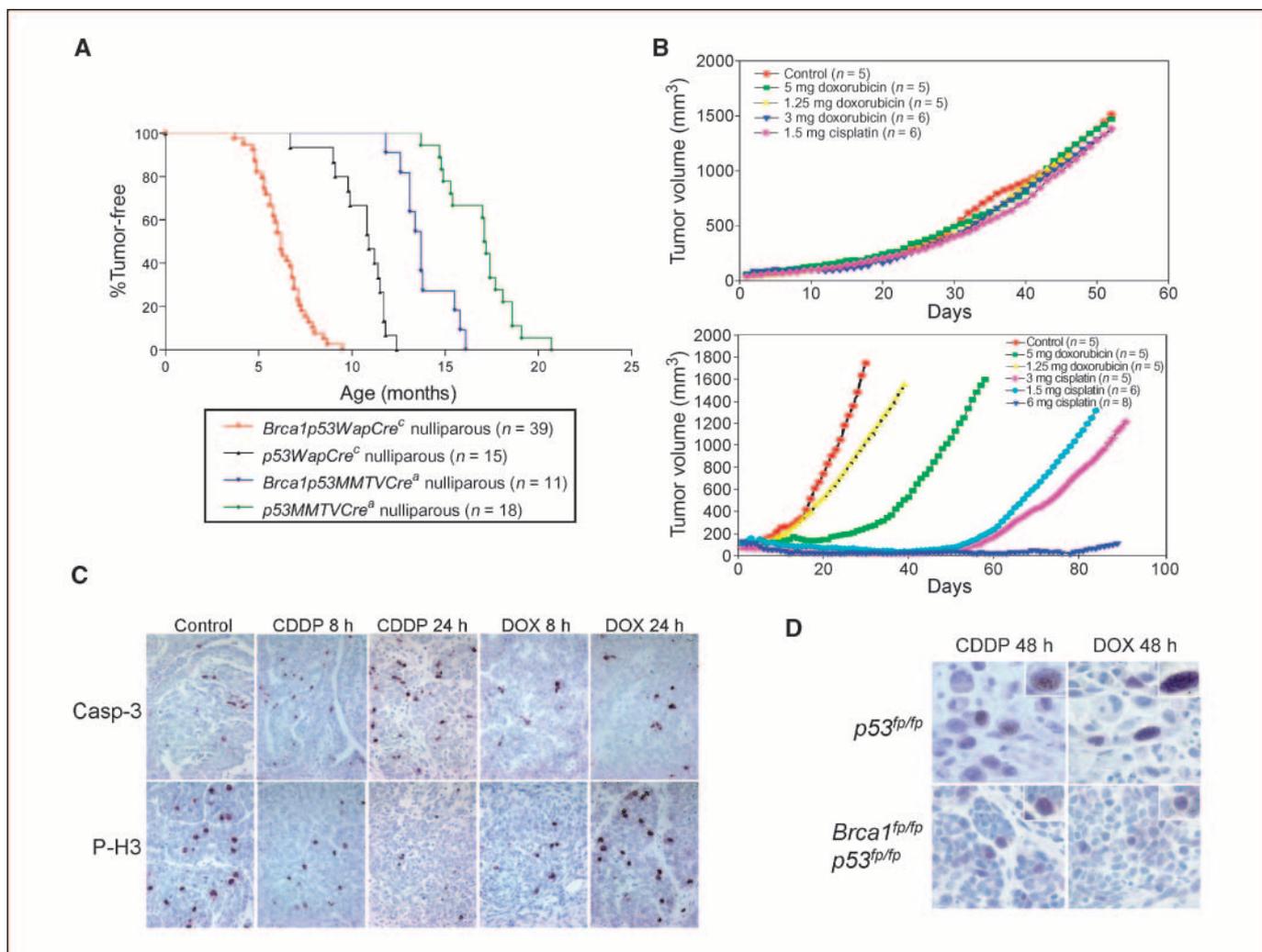
Figure 1. *Brca1/p53*–mediated mammary tumors are sensitive to cisplatin treatment. *A,* proportion of tumor-free nulliparous *Brca1^fp/fp^p53^fp/fp^* and *p53^fp/fp^;Cre* mice. *X axis,* age of each mouse when a palpable tumor was first detected. The curves were plotted using the Kaplan-Meier method. *n* values indicate the number of mice analyzed of each genotype. *B,* response of *p53*-mediated (*top*) and *Brca1/p53*–mediated (*bottom*) mammary tumors to doxorubicin or CDDP *in vivo*. Data were obtained using both *WAPCre^c^* and *MMTVCre^a^* mice. Tumor growth was monitored by taking daily caliper measurements in two perpendicular dimensions as described in Materials and Methods. *C,* immunohistochemical staining of activated caspase-3 (*Casp-3*) and phospho-histone 3 (*P-H3*) in CDDP- or doxorubicin (*DOX*)-treated samples at the indicated time points. *D,* Rad51 foci formation in CDDP- or doxorubicin-treated tumors. *Insets,* higher magnifications of stained nuclei. A total of 8 *Brca1/p53*–mediated and 10 *p53*-mediated tumors were analyzed, and all showed similar results.

treatment was done in three mice (Fig. 2*A* and data not shown). Tumor shrinkage was observed initially but tumors recurred with a more rapid growth rate than the original relapsed tumor following 1 week of complete regression (Fig. 2*A*). Rapid recurrence and growth suggest the existence of a subpopulation of cisplatin-resistant cells and selection of the resistant cells during successive platinum treatment.

Previous studies have shown that cancer stem cells contribute to cancer recurrence and chemoresistance in several tumor types. To investigate whether cancer stem cells contribute to platinum resistance, we first tested whether markers for normal mammary stem cells could be used to enrich mammary cancer stem cells. CD24, a heat-stable antigen, is expressed in human breast tumors and neural stem cells. Sleeman and colleagues (28) divided the CD24-expressing normal mammary cells into three subgroups (i.e., $CD24^{low}$, $CD24^{med}$, and $CD24^{hi}$) and showed that cells with the highest repopulation capacity resided in the $CD24^{med}$ population. CD29 (β_1-integrin), a stem cell marker in skin, was found to be

expressed at a very high level in normal mouse mammary stem cells (25). Thus, we characterized the $CD29^{hi}CD24^{med}$ cells that represented 3.8% to 8.0% (mean, 5.9%) of tumor cell population in primary tumors that arose following CDDP treatment (Fig. 2*B*). Cells analyzed from untreated primary tumors had a mean of 1.5% $CD29^{hi}CD24^{med}$ cells (data not shown). Injections of 1,000 (5 of 5) and 500 (4 of 6) $CD29^{hi}CD24^{med}$ cells from the resistant primary tumors into fat pads of immunodeficient mice gave rise to tumors, whereas injections of 1,000 $CD29^{med}24^{hi}$ cells (0 of 4) did not (Fig. 2*C*). One of five injections of $CD29^{med}24^{-/lo}$ resulted in small tumors. This is perhaps due to the presence of small numbers of contaminating cells from the $CD29^{hi}CD24^{med}$ population. Alternatively, the $CD29^{med}24^{-/lo}$ population may contain a small number of cells with limited proliferative ability. Thus, cancer cells expressing high level of CD29 and intermediate level of CD24 are more likely to represent the cancer stem cell subpopulation because they showed a greater repopulation capacity than $CD29^{med}24^{-/lo}$ or $CD29^{med}24^{hi}$. In the normal mammary fat pad,

a single CD29^{hi}CD24$^+$ cell is capable of reconstituting a functional mammary gland (25). Importantly, the CD29^{hi}CD24^{med} cells give rise to tumors that express a wide range of CD29 and CD24 (Fig. 2D).

To systematically investigate the role of CD29^{hi}CD24^{med} cells in cisplatin resistance, we investigated whether tumors that developed in *Rag1*$^{-/-}$ mice, following transplantation of FACS-sorted tumor cells, respond to platinum treatment. Treatment of first-round primary transplants (*n* = 10) resulted only in partial regression (Fig. 3A, *dotted line*). Importantly, secondary tumor transplants (*n* = 7) generated from CD29^{hi}CD24^{med} cells were completely refractory to CDDP treatment (Fig. 3A, *solid line*), suggesting an increase in CDDP-resistant cells compared with the primary transplant tumor. Rottenberg and colleagues (29) reported that they were unable to identify resistance to CDDP when they performed transplantations using tumor pieces. They, however, also failed to eliminate the tumors, suggesting the potential existence of CDDP-resistant, tumor-initiating cells. In our study, we showed that these cells are enriched in the CD29^{hi}24^{med} subpopulation. To test whether there were expansions of these cancer stem cells, we compared profiles of CD29 and CD24 in tumor cells from the primary and secondary tumor transplants. The frequency of CD29^{hi}CD24^{med} cells ranged from 6.6% to 11.0% (mean, 8.8%; *n* = 10) in the primary transplants and from 16.5% to 29.2% (mean, 22.8%, *n* = 7) in the secondary tumor transplants (Fig. 3B and data not shown). Thus, there is an ∼3-fold increase in the frequency of CD29^{hi}CD24^{med} cells in the secondary tumor transplants compared with the primary transplants, suggesting that the expansion of the CD29^{hi}CD24^{med} population may contribute to platinum resistance. Because frequencies of CD29^{hi}CD24^{med} cell populations in primary transplants are comparable to those in recurrent and primary tumors,

it is unlikely that expansion of these populations in the secondary tumor transplants is due to transplantation per se. To confirm this, we carried out FACS analysis on primary and secondary transplant tumors that were not treated with CDDP. Results showed that the percentage of CD29^{hi}CD24^{med} in these tumors remained low, within the range of 3.5% to 9.8% (mean, 6.6%; *n* = 5). Importantly, in the CDDP-treated tumors, the CD29^{hi}CD24^{med} cells gave rise to heterogeneous cell populations, expressing wide ranges of CD24 and CD29 (Fig. 3B), indicating that the regenerated tumors contained phenotypically diverse populations of cells, as one would expect from cancer stem cells.

In addition to assaying the potential of cancer stem cells to regenerate tumors *in vivo*, we also carried out *in vitro* colony-forming assays on CD29^{hi}CD24^{med} cells. Colony formation assay has previously been used for estimation of progenitor numbers in a cell population (23–25). CD29^{hi}CD24^{med} cells have ∼3- and 6-fold higher colony-forming efficiencies on irradiated NIH 3T3 feeder layers than CD29^{med}24$^{-/lo}$ and CD29^{med}24^{hi} cells, respectively (Fig. 3C). In a separate experiment, a low colony-forming ability was seen with unsorted cells (Fig. 3D, *shaded column*). These independent experiments provided further evidence that the CD29^{hi}CD24^{med} population contained higher numbers of mammary progenitor cells. In the unsorted population, cells harvested from the second transplant were 3-fold enriched for colony formation compared with cells from the first transplant (Fig. 3D). This observation corroborates the findings from the FACS analyses where a 3-fold increase in the CD29^{hi}CD24^{med} subpopulation was observed in the secondary transplant. These colonies were also larger (Fig. 3D, *bottom*), suggesting increased proliferation of cancer stem cells following secondary transplantation. To explore the possibility that this population of cells were also CDDP resistant, we added CDDP at

Figure 2. Chemoresistance to CDDP *in vivo* and the presence of cancer stem cells. *A,* sensitivity of primary and recurrent mammary tumors to CDDP treatment. CDDP was administered i.p., when tumors reached ∼0.5 cm³, at 0.5 mg/kg daily for 7 d. Tumor sizes were monitored following detection of palpable tumors before, during, and after CDDP treatment (*n* = 8). Tumor that recurred in three mice underwent additional cycle of treatments. *B,* FACS sorting analyses done on cells dissociated from primary tumor. Cells sorted according to the indicated gatings were used for *in vivo* tumorigenicity assays. *C,* transplantation using 1,000 cells of the CD29^{hi}CD24^{med} subpopulation resulted in tumor formation (*arrows*) whereas CD29^{med}24$^{-/lo}$ (*arrowhead*) or CD29^{med}24^{hi} (*asterisk*) did not. *D,* a representative FACS profile of the resulting tumors following CD29^{hi}CD24^{med} cell transplantations.
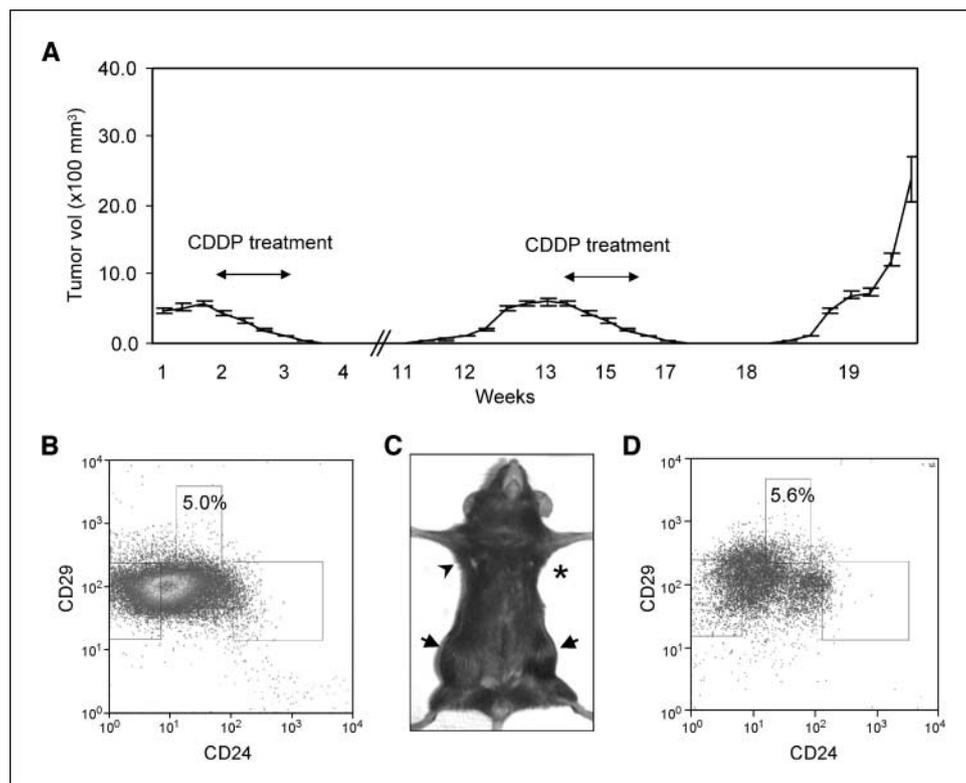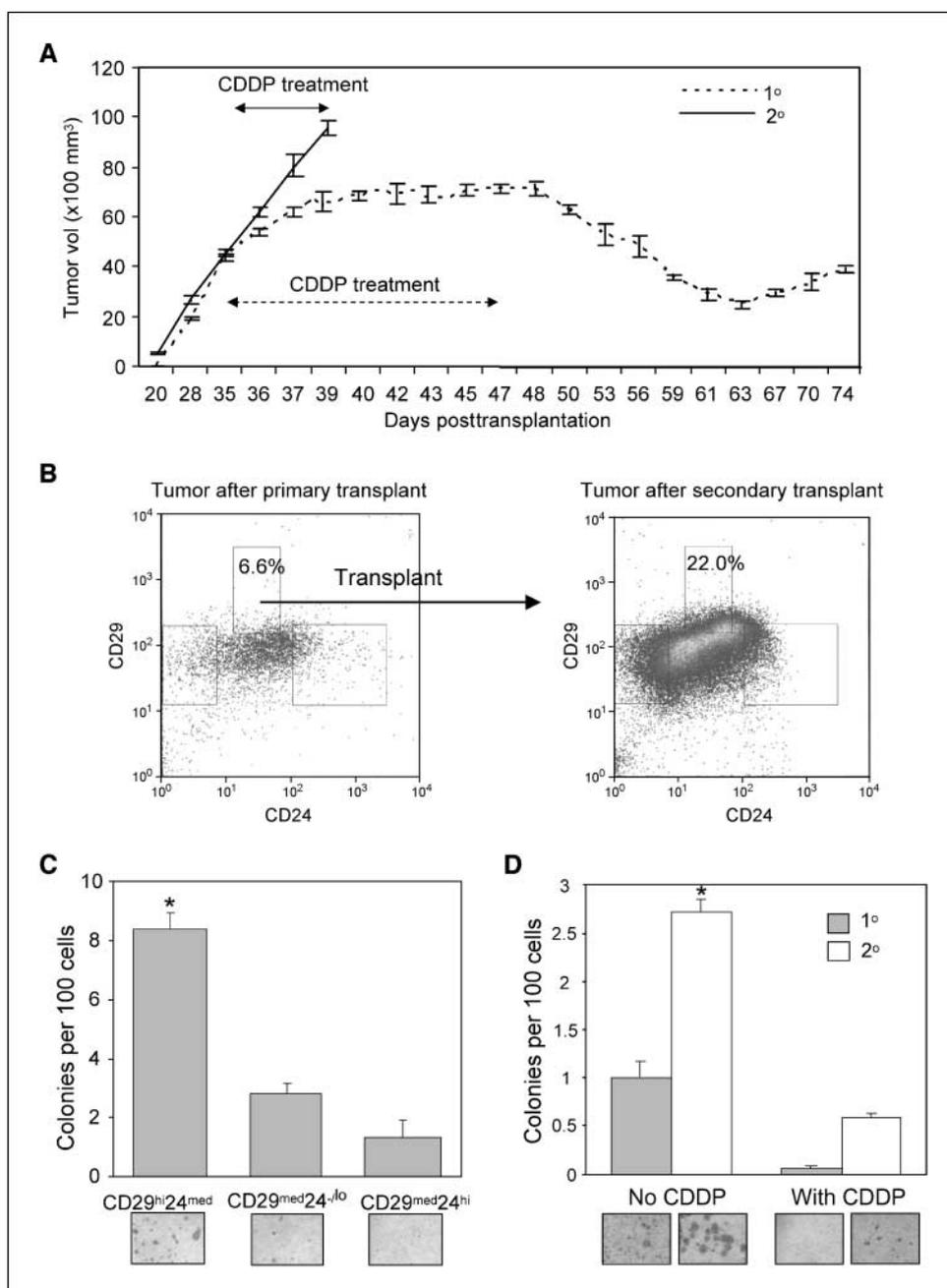
Figure 3. Chemoresponse, FACS profiling, and colony-forming abilities of the primary and secondary Brca1[fp/fp]p53[fp/fp] tumor transplants. A, response to CDDP treatment of the primary and secondary tumor transplants, developed after transplantation with 1,000 CD29^{hi}CD24[med] cells. The treatment was administered i.p., when tumors reached ~0.5 cm^3, at 0.5 mg/kg daily for 7 d. Tumor volumes before, during, and after CDDP treatment were shown. Arrows are not drawn to scale. B, FACS analyses of cells dissociated from primary tumor transplant, which showed partial resistance to CDDP (left), and from secondary tumor transplant, which were refractory to CDDP (right). C, colony formation assay of sorted CD29^{hi}CD24[med], CD29[med]24[−/lo], and CD29[med]24^{hi} cells from the primary tumor transplant. D, colony formation of unsorted cells from primary and secondary tumor transplants in the presence or absence of CDDP. C and D, columns, mean number of colonies per 100 primary cells; bars, SD. *, $P < 0.05$, versus the control group.

a predetermined GI$_{50}$ concentration to the culture in the colony assay. Interestingly, ~22% of the colonies from the second transplant were resistant to CDDP treatment, compared with <1% from the first transplant (Fig. 3D), strongly suggesting an expansion of CDDP-resistant progenitor cells in the second transplant population.

To investigate the involvement of key regulators in self-renewal and pluripotency in these CD29^{hi}CD24[med] populations, we carried out semiquantitative RT-PCR for Nanog, Oct4, and Sox2, critical players for the pluripotent embryonic stem cells (reviewed in ref. 30). Sox2 and Oct4 expression was low in all the samples from primary as well as secondary tumor transplants, whereas Oct4 expression was readily detectable in the embryonic stem cells (Fig. 4A and B). Interestingly, Nanog was readily detectable in these cells, particularly in the primary tumor transplant, whereas

Nanog expression was reduced in CD29^{hi}CD24[med] populations of the secondary tumor transplants. Lin and colleagues (31) showed that Nanog expression is suppressed by p53, leading to mouse embryonic stem cell differentiation. In our mouse model, conditional deletion of p53 may contribute to Nanog up-regulation. On the other hand, in contrast to normal stem cells, Nanog may no longer be subject to Sox2-Oct4 transcriptional regulation in cancer stem cells.

We also examined MDR1 and Top2A expression in primary and secondary tumor transplants by semiquantitative RT-PCR. MDR1 expression was low or below detection in all cases (Fig. 4A). However, whereas high levels of Top2A expression were seen in primary transplants, expression was greatly reduced in all secondary transplants examined (Fig. 4A and data not shown). Genomic deletion of Top2A was seen in one of the secondary

tumors (Fig. 4C). Whereas differential gene expression was detected in primary and secondary tumor transplants, mechanisms leading to chemoresistance remain to be addressed. It should be noted that down-regulation of *Top2A* has been observed in postchemotherapy samples compared with the primary tumors (32), suggesting its possible contribution to chemoresistance. However, it should also be noted that expression of *Top2A* has been associated with both cisplatin resistance and sensitivity in ovarian cancer in different studies (33, 34). Therefore, the predictive power of *Top2A* in BRCA1-associated tumors has yet to be elucidated.

Taken together, exposure to CDDP may lead to the emergence of a subpopulation of mouse tumor cells (i.e., CD29^{hi}CD24^{med}) that become resistant to CDDP (Fig. 4D). Alternatively, a small population of preexisting cells with inherent CDDP resistance survives CDDP treatment. Following subsequent exposure to CDDP, these resistant cells self-renew as well as differentiate into tumor masses containing cells of various phenotypes. Transplantation of this subpopulation of cells into immunodeficient mice led to its further expansion. Up-regulation of *c-Myc* was detected in the CD29^{hi}CD24^{med} population in the primary, but not secondary, tumor transplant. Whether c-myc and Nanog are involved in the expansion, but not maintenance, of the CD29^{hi}CD24^{med} cancer stem cell populations remains to be addressed.

Studies by Rottenberg and colleagues (29) used a model with null alleles of *Brca1* and *p53*, whereas the model described here expressed exon 11–less isoforms of *Brca1*. The CDDP treatment regimen also differs in the two studies. A 20-day recovery preceded each single injection of CDDP reported by Rottenberg and colleagues (29). Tumors were not eliminated under the regimen, indicating the existence of chemoresistant cells. The spontaneous chemoresistant model described here allows a longitudinal follow-up of putative
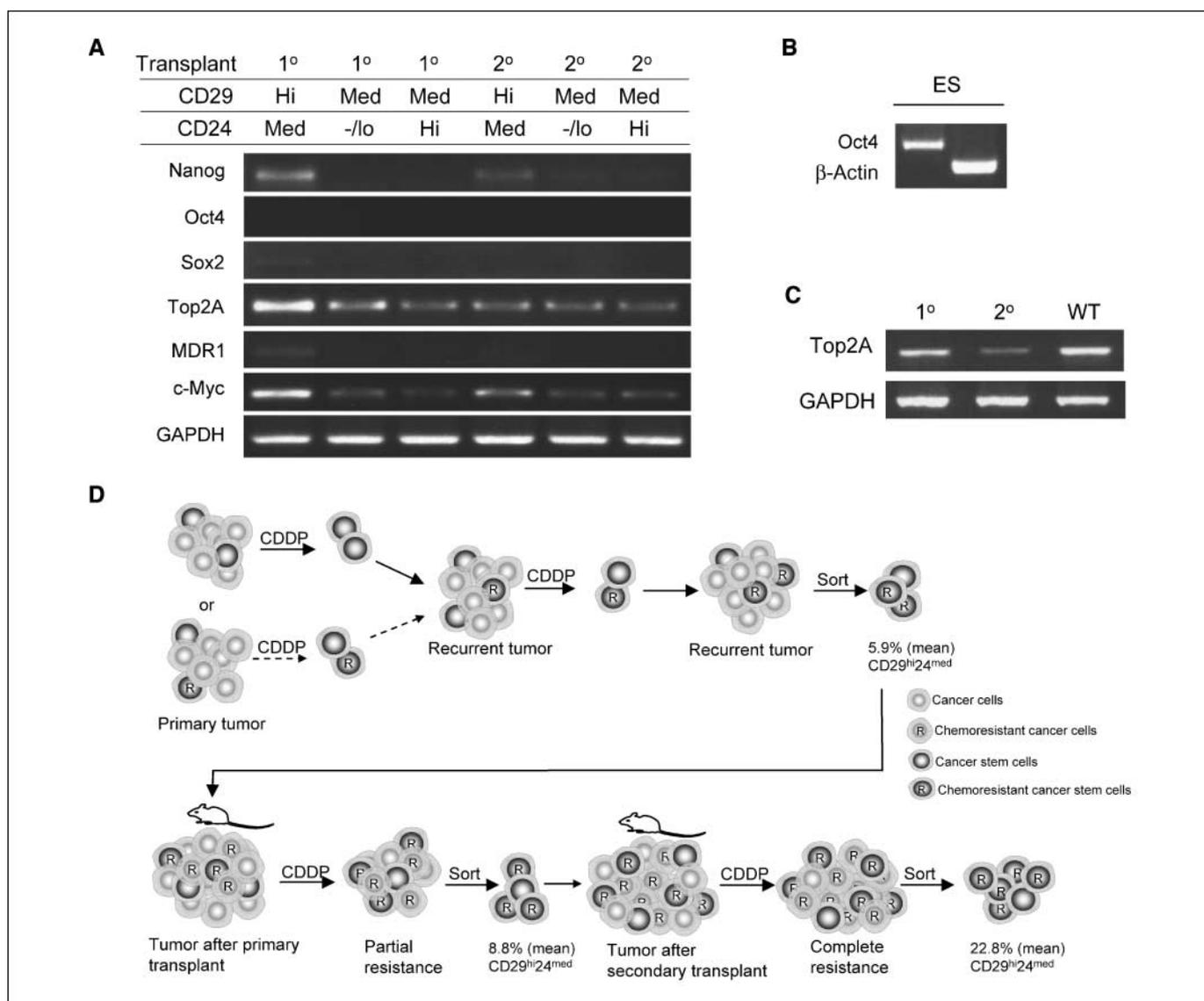

Figure 4. Selective gene expression profiles in recurrent primary and secondary tumor transplants. *A,* semiquantitative RT-PCR analyses of CD29^{hi}CD24^{med}, CD29^{med}24$^{-/lo}$, and CD29^{med}24^{hi} cells from the primary and secondary tumor transplants. *B,* a positive control for Oct4, using mouse embryonic stem (*ES*) cells. *C,* semiquantitative PCR analyses of genomic DNA of CD29^{hi}CD24^{med} cells from the primary and secondary tumor transplants; *WT,* wild-type. *D,* model illustrating changes in cancer stem cells during the course of chemotherapy.

cancer stem cells that will allow delineation of chemoresistance. Clearly, the platinum-resistant CD29^{hi}CD24^{med} cancer stem cells not only expanded but presumably also increased their proliferation rates relative to the total population of tumor cells during the treatment course.

Disclosure of Potential Conflicts of Interest

No potential conflicts of interest were disclosed.

References

1. Antoniou AC, Easton DF. Models of genetic susceptibility to breast cancer. Oncogene 2006;25:5898–905.
2. Walsh T, King MC. Ten genes for inherited breast cancer. Cancer Cell 2007;11:103–5.
3. Esteller M, Silva JM, Dominguez G, et al. Promoter hypermethylation and BRCA1 inactivation in sporadic breast and ovarian tumors. J Natl Cancer Inst 2000;92:564–9.
4. Ting NS, Lee WH. The DNA double-strand break response pathway: becoming more BRCAish than ever. DNA Repair (Amst) 2004;3:935–44.
5. Turner N, Tutt A, Ashworth A. Hallmarks of "BRCAness" in sporadic cancers. Nat Rev Cancer 2004;4:814–9.
6. Heine GF, Parvin JD. BRCA1 control of steroid receptor ubiquitination. Sci STKE 2007;391:pe34.
7. Sorlie T, Perou CM, Tibshirani R, et al. Gene expression patterns of breast carcinomas distinguish tumor subclasses with clinical implications. Proc Natl Acad Sci U S A 2001;98:10869–74.
8. Gruvberger-Saal SK, Persson C, Lövgren K, et al. Recurrent gross mutations of the PTEN tumor suppressor gene in breast cancers with deficient DSB repair. Nat Genet 2008;40:102–7.
9. Farmer H, McCabe N, Lord CJ, et al. Targeting the DNA repair defect in BRCA mutant cells as a therapeutic strategy. Nature 2005;434:917–21.
10. Bhattacharyya A, Ear US, Koller BH, Weichselbaum RR, Bishop DK. The breast cancer susceptibility gene BRCA1 is required for subnuclear assembly of Rad51 and survival following treatment with the DNA cross-linking agent cisplatin. J Biol Chem 2000;275:23899–903.
11. Tassone P, Tagliaferri P, Perricelli A, et al. BRCA1 expression modulates chemosensitivity of BRCA1-defective HCC1937 human breast cancer cells. Br J Cancer 2003;88:1285–91.
12. Lin SC, Lee KF, Nikitin AY, et al. Somatic mutation of p53 leads to estrogen receptor α-positive and -negative

mouse mammary tumors with high frequency of metastasis. Cancer Res 2004;64:3525–32.
13. Poole AJ, Li Y, Kim Y, Lin SC, Lee WH, Lee EY. Prevention of Brca1-mediated mammary tumorigenesis in mice by a progesterone antagonist. Science 2006;314:1467–70.
14. Liu X, Holstege H, van der Gulden H, et al. Somatic loss of BRCA1 and p53 in mice induces mammary tumors with features of human BRCA1-mutated basal-like breast cancer. Proc Natl Acad Sci U S A 2007;104:12111–6.
15. Xu X, Wagner KU, Larson D, et al. Conditional mutation of Brca1 in mammary epithelial cells results in blunted ductal morphogenesis and tumour formation. Nat Genet 1999;22:37–43.
16. Kelland L. The resurgence of platinum-based cancer chemotherapy. Nat Rev Cancer 2007;7:573–84.
17. Tack DK, Palmieri FM, Perez EA. Anthracycline vs nonanthracycline adjuvant therapy for breast cancer. Oncology 2004;18:1367–76.
18. Reya T, Morrison SJ, Clarke MF, Weissman IL. Stem cells, cancer, and cancer stem cells. Nature 2001;414:105–11.
19. Clarke MF, Fuller M. Stem cells and cancer: two faces of eve. Cell 2006;124:1111–5.
20. Al-Hajj M, Wicha MS, Benito-Hernandez A, Morrison SJ, Clarke MF. Prospective identification of tumorigenic breast cancer cells. Proc Natl Acad Sci U S A 2003;100:3983–8.
21. Liu G, Yuan X, Zeng Z, et al. Analysis of gene expression and chemoresistance of CD133+ cancer stem cells in glioblastoma. Mol Cancer 2006;5:67–78.
22. Gutova M, Najbauer J, Gevorgyan A, et al., Identification of uPAR-positive chemoresistant cells in small cell lung cancer. PLoS ONE 2007;2:e243.
23. Stingl J, Emerman JT, Eaves CJ. Enzymatic dissociation and culture of normal human mammary tissue to detect progeny activity. In: Helgason CD, Miller CL, editors. Methods in molecular biology: basic cell culture protocols. New Jersey: Humana; 2005. p. 249–63.

24. Stingl J, Eirew P, Ricketson I, et al. Purification and unique properties of mammary epithelial stem cells. Nature 2006;439:993–7.
25. Shackleton M, Vaillant F, Simpson KJ, et al. Generation of a functional mammary gland from a single stem cell. Nature 2006;439:84–8.
26. Skarnes WC. Gene trapping methods for the identification and functional analysis of cell surface proteins in mice. Methods Enzymol 2000;328:592–615.
27. Bartz SR, Zhang Z, Burchard J, et al. Small interfering RNA screens reveal enhanced cisplatin cytotoxicity in tumor cells having both BRCA network and TP53 disruptions. Mol Cell Biol 2006;26:9377–86.
28. Sleeman KE, Kendrick H, Ashworth A, Isacke CM, Smalley MJ. CD24 staining of mouse mammary gland cells defines luminal epithelial, myoepithelial/basal and non-epithelial cells. Breast Cancer Res 2006;8:R7.
29. Rottenberg S, Nygren AO, Pajic M et al. Selective induction of chemotherapy resistance of mammary tumors in a conditional mouse model for hereditary breast cancer. Proc Natl Acad Sci U S A 2007;104:12117–22.
30. Boiani M, Scholer HR. Regulatory networks in embryo-derived pluripotent stem cells. Nat Rev Mol Cell Biol 2005;6:872–84.
31. Lin T, Chao C, Saito S, et al. p53 induces differentiation of mouse embryonic stem cells by suppressing Nanog expression. Nat Cell Biol 2005;7:165–71.
32. Jazaeri AA, Awtrey CS, Chandramouli GV, et al. Gene expression profiles associated with response to chemotherapy in epithelial ovarian cancers. Clin Cancer Res 2005;11:6300–10.
33. Helleman J, Jansen MPHM, Span PN, et al. Molecular profiling of platinum resistant ovarian cancer. Int J Cancer 2005;118:1963–71.
34. Cornarotti M, Capranico G, Bohm S, et al. Gene expression of topoisomerase I, IIα and IIβ and response to cisplatin-based chemotherapy in advanced ovarian carcinoma. Int J Cancer 1996;67:479–84.

Cancer Stem Cells Contribute to Cisplatin Resistance in *Brca1/p53*–Mediated Mouse Mammary Tumors

Norazizah Shafee, Christopher R. Smith, Shuanzeng Wei, et al.

Updated version	Access the most recent version of this article at: http://cancerres.aacrjournals.org/content/68/9/3243
Supplementary Material	Access the most recent supplemental material at: http://cancerres.aacrjournals.org/content/suppl/2008/04/28/68.9.3243.DC1

Cited articles	This article cites 33 articles, 9 of which you can access for free at: http://cancerres.aacrjournals.org/content/68/9/3243.full#ref-list-1
Citing articles	This article has been cited by 32 HighWire-hosted articles. Access the articles at: http://cancerres.aacrjournals.org/content/68/9/3243.full#related-urls

E-mail alerts	Sign up to receive free email-alerts related to this article or journal.
Reprints and Subscriptions	To order reprints of this article or to subscribe to the journal, contact the AACR Publications Department at pubs@aacr.org.
Permissions	To request permission to re-use all or part of this article, use this link http://cancerres.aacrjournals.org/content/68/9/3243. Click on "Request Permissions" which will take you to the Copyright Clearance Center's (CCC) Rightslink site.